Image Improvement Through Metamaterial Technology for Brain Stroke Detection

Olympia Karadima, Eleonora Razzicchia, Panagiotis Kosmas
Department of Engineering, Kings College London, London, UK, Email: panagiotis.kosmas@kcl.ac.uk

***Abstract*—In this paper we investigate the capabilities of metamaterials technology to enhance the quality of reconstructed images for the problem of brain stroke detection. We integrate the metamaterial in our headband system for brain imaging in CST, and evaluate the reconstructed images of the head model that is placed inside the microwave tomographic head system for the cases with and without the incorporated metamaterial. For image reconstruction we apply the distorted Born iterative method (DBIM) combined with two-step iterative shrinkage/thresholding (TwIST) algorithm. Our results indicate that the use of our metamaterial can increase the signal difference due to the presence of a blood target, which translates into more accurate reconstructions of the target.**

***Index Terms*—microwave imaging, metamaterials, DBIM, TwIST.**

I. Introduction

Brain stroke is a serious condition that occurs when a part of the brain is either blocked (ischemic) or burst (hemorrhagic). Treatment depends on the cause and the part of the brain that is affected. As a result, the patient's survival heavily depends on the successful and early detection of the type of stroke, since a wrong or delayed treatment could be proven fatal. In this framework, there is the need for a quick, cost-effective and portable method of imaging [1].

Microwave tomographic (MWT) methods rely on the existing difference between the dielectric properties of healthy and malignant tissues. Through solving an inverse, ill-posed electromagnetic (EM) scattering problem, a map of the spatial distribution of the dielectric properties of the region of interest is reconstructed, allowing to locate a target with unknown properties [2]. The use of non-ionizing radiation, portability and the low cost of this system are the main motivations that have established MWT as a promising alternative to current imaging techniques [3].

A valid MWT scanner for brain imaging should maximize the incident power penetrating into the human head. Thus, compact antennas operating below 1.5 GHz immersed in a coupling medium are used [4]. Structures such as helmet or chambers, allow the use of a lossy dielectric medium for the operating antennas [5], [6]. Nevertheless, the success of a MWT device depends on the hardware characteristics in conjunction with a strong and robust imaging algorithm. An implementation of the distorted Born iterative method (DBIM) combined with a two-step iterative shrinkage/thresholding method (TwIST) has been developed in [7], [8] and further tested in [9] and [10]. To increase the penetration depth into the lossy tissues and secure adequate spatial resolution images, electrically thin metamaterials (MM) might be used to couple the incident power into the region of interest of the human body. MMs exhibit strong enhancement of fields which may lead to an improvement of sensors' sensitivity and introduce more freedom in sensing design [11]. These MM structures are mainly based on split-ring resonators (SRRs), which present several advantages such as the high flexibility of their design process [12].

In previous studies, we have examined various aspects of our work towards the design of a MWT scanner for brain imaging which incorporates a MM layer for signal enhancement and the DBIM-TwIST algorithm for recovering the unknown target of interest [13]–[15]. This paper examines in more details the potential of improving the quality of the reconstructed images for stroke detection and monitoring, by integrating MM technology in our MWT scanner. The SRR-based MM film is shown to improve the overall sensitivity of the MWT system, which translates into reduction of artefacts in the reconstructed images.

Next section provides a summary of our DBIM-TwIST algorithm and presents the MM design along with the simulation setup. Section III discusses the reconstruction results using DBIM-TwIST approach, which illustrate the advantages of the integrated MM, followed by a Conclusion section.

II. METHODS

A. Distorted Born Iterative Method (DBIM)

DBIM is an iterative inverse algorithm that reconstructs a map of the spatial distribution of the dielectric properties within a region of interest, by solving a nonlinear inverse EM scattering problem [16]. The nonlinear and ill-posed equation, which describes the relationship of the electric field with the continuous spatial distribution of dielectric properties, can be discretized under the Born approximation:

$$\begin{aligned} E_s(r_n, r_m) &= E(r_n, r_m) - E_b(r_n, r_m) \\ &= \omega^2 \mu \int_V G_b(r_n, r) E_b(r, r_n)(\epsilon(r) - \epsilon_b(r) dr) \end{aligned} \tag{1}$$

where E, E_s and E_b are the total, scattered and background fields respectively. The complex permittivity of the known background and unknown object is indicated as $\epsilon_b(r)$ and $\epsilon(r)$ respectively, and their difference is the contrast function $O(r)$. The Green's function is estimated as follows:

$$G_b = \frac{i}{\omega \mu} E_b \tag{2}$$

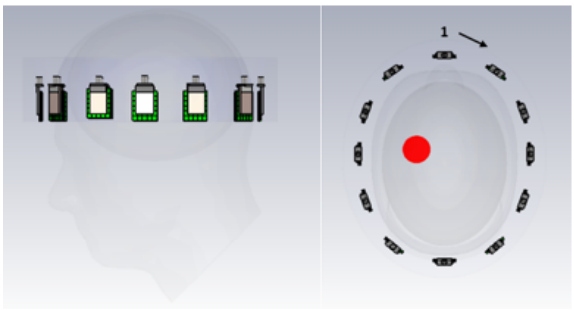

Fig. 1. Head model and headband system geometry. The array consists of 12 spear patch antennas printed on a FR-4 substrate. The MM is placed adjacent to the antenna's substrate.

Therefore, by (1) and (2) the nonlinear integral equation at each iteration is discretized into:

$$E_s(r_n, r_m) \approx \iota\omega \int_V E_b(r, r_m) E_b(r, r_n) O(r) dr \qquad (3)$$

which is translated into a linear but ill-posed EM problem [7] that can be solved by the TwIST method, based on the algorithm presented in [17]. More specifically, TwIST solves the ill-posed linear system,

$$Ax = y \qquad (4)$$

at each DBIM iteration. It estimates the unknown vector x, from the observation vector y, by splitting the matrix in a two-step iterative equation. The next estimated solution depends on the current solution as well as previous solution. Solving towards vector x, the background properties are calculated and updated iteratively, and hence the reconstruction of the domain based on the values of the permittivity and conductivity is achieved. The main advantage of the DBIM-TwIST compared to other inverse ill-posed problem solvers, relies on the shrinkage/thresholding adaptive operators [7].

B. Simulation Setup

A novel MM design was incorporated in our system for brain imaging. Fig. 1 shows the scanner, consisting of a 12-antenna elliptical array placed inside a headband filled with a 90% glycerol-water mixture [15]. The scanner was tested using the EN 50361 Specic Anthropomorphic Mannequin (SAM) head model, including average brain tissue (ε = 45.8; σ = 0.76 S/m) inside a skull layer (ε = 20; σ = 0.35 S/m). We refer to this configuration as the "no target" scenario. We have also studied this setup in the presence of a target resembling a blood-clot inside the brain volume ("target" scenario). The target consists of a cylinder with 2 cm height and 3 cm diameter, located in the front-left part of the brain. We assigned dielectric properties of blood from CST's library (ε = 61.0; σ = 1.56 S/m at 1.0 GHz). A MM layer (24.75 mm $\times$ 29.7 mm), whose unit cell is illustrated in Fig. 2, was placed on each antenna, adjacent to the substrate. The MM unit cell comprises a metallic lattice embedded between two Rogers 3010 TM substrates. The metallic pattern (thickness = 0.10 mm) is a variation of the Jerusalem Cross SRR. Our previous

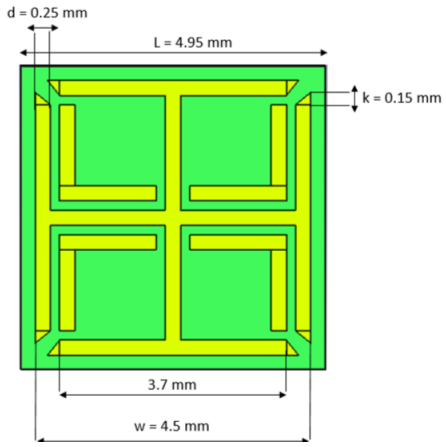

Fig. 2. Square unit cell MM, comprising a copper lattice placed between two Rogers 3010 TM substrates (thickness = 1.27 mm, ϵ = 10.2 and tanδ = 0.0022).

studies have already shown the MM unit cell design and the performance of MM layers based on this structure [13], [14].

C. Forward model

To validate our hypothesis, we assessed the effect of the integrated MM by generating reconstructed images using the DBIM-TwIST. Data obtained from the same "target - no target" CST simulations for two cases (with and without the MM). The algorithm uses the finite-difference time-domain (FDTD) method as a forward solver in a two-dimensional (2-D) simplified model of the simulation. The forward model consists of an elliptical two-layer geometry which simulates the skull and the brain, inserted in a tank filled with 90% glycerol-water mixture with line sources in an elliptical array, placed in the same locations as the antennas of the CST simulation. We point out that the forward model does not include the MM design and the reconstruction domain comprises only the simplified 2-D head with dimensions of 170 $\times$ 205 mm. To consider the dispersive behaviour of the human tissues and the matching medium, we used the first-order Debye model for the average brain, skull and 90% glycerol-water mixture, respectively. Debye parameters are then used for reconstructing the dielectric properties inside the reconstruction area [16]. We implemented DBIM-TwIST algorithm for both single frequency and frequency hoping at 0.8, 1.5 and 2.0 GHz. Frequency hopping approach is explained in detail in [18].

III. RESULTS

The transmission parameters were calculated via CST simulations over the 0.5-2.0 GHz frequency range for the antenna's resonant frequency (1.5 GHz), and the signal difference "target - no target"(dB), with and without the MM, was calculated. Fig. 3 plots the difference "target - no target" (dB), which was obtained in the presence of the MM and the signal difference "target - no target" that calculated without the MM. These two differences are plotted as a function of the receiver location

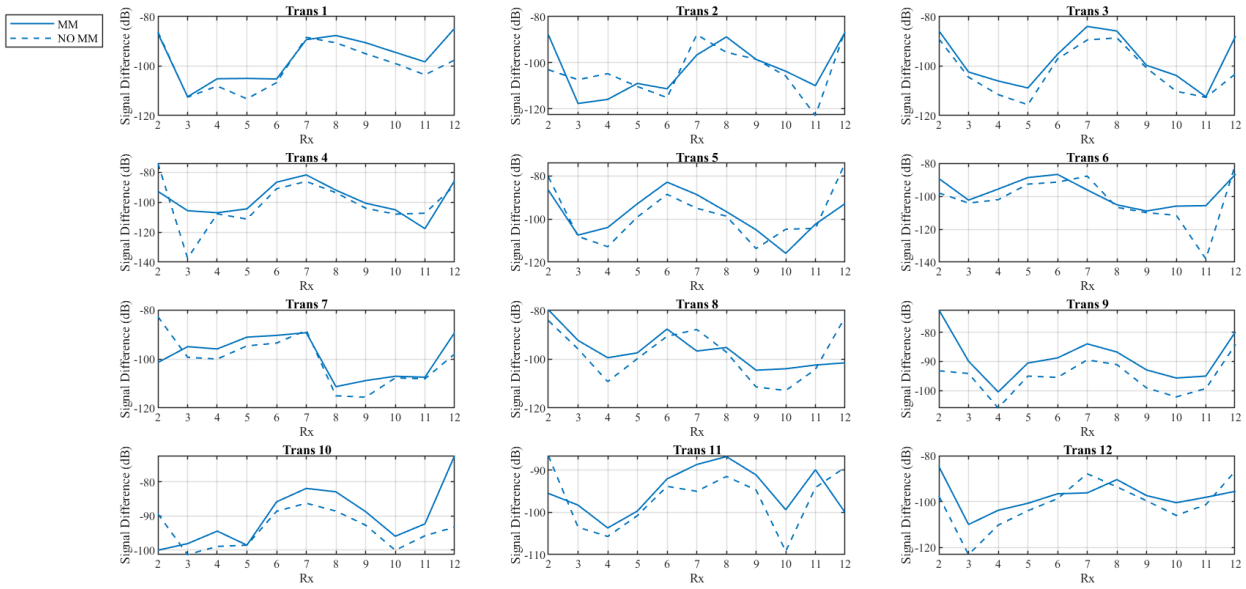

Fig. 3. Signal difference "target - no target" (in dB) with the MM (solid lines) and without the MM (dashed lines) as a function of receiver location.

at 1.5 GHz. We observe that the MM layer has the ability of enhancing the EM field when placed close to the antennas, increasing the level of the signal due to the blood-like target inside the brain. For instance, considering transmitter 9 (Trans 9), the difference between the function "target - no target" in the presence of the MM and the function "target - no target" without the MM is 25 dB for receiver 2.

Fig. 4 presents the reconstructed permittivity, obtained with DBIM-TwIST algorithm, for the domain inside the antenna array illustrated in Fig. 1. The real part of permittivity at 1.5 GHz was calculated to be ε = 53.83 and ε = 48.24 without and with the intergrated MM, respectively. The results are encouraging, confirming that the use of the MM structure can improve the quality of the reconstructed image and reduce the artefacts. However, for the case without the integration of MM, calculated values of permittivity are slightly increased and closer to the actual values of target's permittivity.

Fig. 5 illustrates the reconstructed permittivities which were obtained using the frequency hopping technique. The real permittivity of the target at 2.0 GHz is ε = 49.16 and ε = 51.74, for the case with and without the MM, respectively. As expected, for both cases the target is better localized due to frequency hopping approach, which uses the data of the previous frequency to reconstruct the properties of the next frequency [7]. It is clear that between the two scenarios, the use of MM improves the quality of the image and produces less artefacts around the target.

IV. CONCLUSIONS

We have studied two different MWT scenarios based on CST simulations, to compare the EM field and the reconstructed images when a MM structure is integrated in a MWT system. The purpose of this study was to examine and

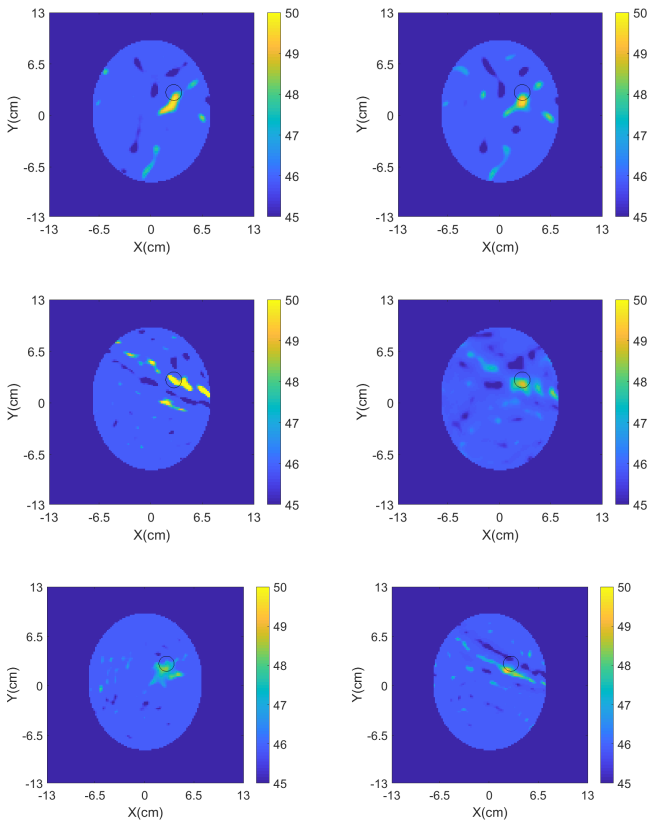

Fig. 4. Reconstructed real part of the complex permittivity for the area inside the antenna ellipsis of Fig. 1 without (left) and with integrated MM (right). The top, middle and bottom rows correspond to permittivity values calculated at 0.8 GHz, 1.5 GHz and 2.0 GHz respectively.

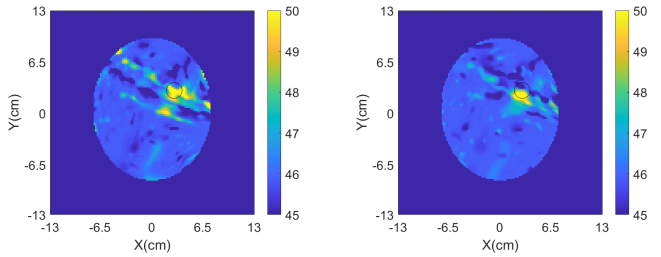

Fig. 5. Reconstructed real part of the complex permittivity for the area inside the antenna ellipsis of Fig. 1 without (left) and with integrated MM (right). The complex permittivity was calculated at 2 GHz using the frequency hopping approach in a frequency range of 0.8-2.0 GHz.

validate the hypothesis that MM technology has the potentials to improve weak signals from targets such as stroke and enhance the quality of the reconstructed images, for brain stroke detection and monitoring. We showed that an increased signal difference due to the presence of the MM leads to higher-quality reconstructions of the blood mimicking target. We note that our model is an oversimplified simulation of the head, however this is a preliminary study and a more rigorous analysis on the impact of the MM on the image reconstructions will be conducted in future research. In the conference we will present a more extended study, including experimental results.

ACKNOWLEDGMENTS

This work was supported by the EMERALD project funded from the European Union's Horizon 2020 research and innovation programme under the Marie Skodowska-Curie grant agreement No. 764479.

REFERENCES

[1] R. C. Heros, "Stroke: early pathophysiology and treatment," Summary of the Fifth Annual Decade of the Brain Symposium., Stroke, vol. 25, no. 9, pp.1877-1881, 1994.

[2] S. Semenov, "Microwave tomography: review of the progress towards clinical applications," Philosophical Transactions of the Royal Society A: Mathematical, Physical and Engineering Sciences, vol. 367, no. 1900, pp. 3021-3042, 2009.

[3] R. Chandra, H. Zhou, I. Balasingham, and R. M. Narayanan, "On the opportunities and challenges in microwave medical sensing and imaging," IEEE transactions on biomedical engineering, vol. 62, no. 7, pp. 1667-1682, 2015.

[4] R. Scapaticci, L. Di Donato, I. Catapano and L. Crocco, "A feasibility study on microwave imaging for brain stroke monitoring," Progress In Electromagnetics Research, vol. 40, pp. 305–324, 2012.

[5] M. Hopfer, R. Planas, A. Hamidipour, T. Henriksson and S. Semenov, "Electromagnetic Tomography for Detection, Differentiation, and Monitoring of Brain Stroke: A Virtual Data and Human Head Phantom Study," IEEE Antennas and Propagation Magazine, vol. 59, no. 5, pp. 86–97, 2017.

[6] J. A. Tobon Vasquez, R. Scapaticci, G. Turvani, G. Bellizzi, N. Joachimowicz, B. Duchêne, E. Tedeschi, M. R. Casu, L. Crocco and F. Vipiana, "Design and Experimental Assessment of a 2D Microwave Imaging System for Brain Stroke Monitoring," International Journal of Antennas and Propagation, vol. 2019, 2019.

[7] Z. Miao and P. Kosmas, "Multiple-frequency DBIM-TwIST algorithm for microwave breast imaging, IEEE Transactions on Antennas and Propagation," vol. 65, no. 5, pp. 2507-2516, 2017.

[8] Z. Miao and P. Kosmas, "Microwave breast imaging based on an optimized two-step iterative shrinkage/thresholding method," in 2015 9th European Conference on Antennas and Propagation (EuCAP), pp. 1-4, 2015.

[9] S. Ahsan, Z. Guo, Z. Miao, I. Sotiriou, M. Koutsoupidou, E. Kallos, G. Palikaras and P. Kosmass, "Design and experimental validation of a multiple-frequency microwave tomography system employing the dbim-twist algorithm," Sensors, vol. 18, no. 10, pp. 3491, 2018.

[10] Z. Guo, S. Ahsan, O. Karadima, I. Sotiriou and P. Kosmas, "Resolution Capabilities of the DBIM-TwIST Algorithm in Microwave Imaging," in 2019 13th European Conference on Antennas and Propagation (EuCAP), pp. 1-4, 2019.

[11] T. Chen, S. Li and H. Sun, "Metamaterials Application in Sensing", Sensors, vol. 12, pp. 2742-2765, 2012.

[12] M. P. Vargas, "Planar Metamaterial Based Microwave Sensor Arrays for Biomedical Analysis and Treatment", Springer Science & Business Media, 2014.

[13] E. Razzicchia, M. Koutsoupidou, H. Cano-garcia, E. Kallos and G. Palikaras, "Metamaterial Designs to Enhance Microwave Imaging Applications," in Proc. 2019 International Conference on Electromagnetics in Advanced Applications (ICEAA), 2019.

[14] E. Razzicchia, I. Sotiriou, H. Cano-garcia, E. Kallos, G. Palikaras and P. Kosmas, "Feasibility Study of Enhancing Microwave Brain Imaging Using Metamaterials," Sensors, vol. 19, no. 24, pp. 5472, 2019

[15] W. Guo, S. Ahsan and P. Kosmas, "Portable Microwave Imaging Head Scanners for Intracranial Haemorrhagic Detection.," in Proc. 2019 Asia-Pacic Microwave Conference (APMC), 2019.

[16] J. D. Shea, P. Kosmas, S. C. Hagness and B. D. Barry, "Three-dimensional microwave imaging of realistic numerical breast phantoms via a multiple-frequency inverse scattering technique," Medical physics, vol. 37, no. 8, pp. 4210-4226, 2010.

[17] J. M. Bioucas-Dias and M. A. Figueiredo,"A new TwIST: Two-step iterative shrinkage/thresholding algorithms for image restoration," IEEE Transactions on Image processing, vol. 16, no. 12, pp. 2992-3004, 2007.

[18] W. C. Chew and J. Lin, "A frequency-hopping approach for microwave imaging of large inhomogeneous bodies," IEEE Microwave and Guided Wave Letters, vol. 5, no. 12, pp. 439-441, 1995.